References and Notes

(1) F. A. Armstrong and A. G. Sykes, *J. Am. Chem. Soc.*, **100**, 7710 (1978).
(2) K. Ogawa, T. Tsukihara, H. Tahara, Y. Katsube, Y. Matsu-ura, N. Tanaka, M. Kakudo, K. Wada, and H. Matsubara, *J. Biochem. (Tokyo)*, **81**, 529 (1977).
(3) B. E. Bryant and W. C. Fernelius, *Inorg. Synth.*, **5**, 188 (1963).
(4) J. C. Bailar and E. M. Jones, *Inorg. Synth.*, **1**, 37 (1959).
(5) R. Davies, M. Mori, A. G. Sykes, and J. A. Weil, *Inorg. Synth.*, **12**, 212 (1970).
(6) The step involving oxidation of $(NH_3)_5CoO_2Co(NH_3)_5^{4+}$ to $(NH_3)_5CoO_2Co(NH_3)_5^{5+}$ was modified slightly: 12 g (not 6 g) of ammonium peroxodisulfate was used, and the resultant solution was left for 30 min.
(7) L. N. Essen, *Inorg. Synth.*, **15**, 93 (1973).
(8) A. L. Oppegard and J. C. Bailar, *Inorg. Synth.*, **3**, 153 (1961).
(9) R. D. Gillard and P. R. Mitchell, *Inorg. Synth.*, **14**, 184 (1972).
(10) F. A. Johnson and E. M. Larsen, *Inorg. Synth.*, **8**, 40 (1966).
(11) See also J. Doyle and A. G. Sykes, *J. Chem. Soc. A*, 795 (1967).
(12) J. K. Beattie and F. Basolo, *Inorg. Chem.*, **10**, 486 (1971).
(13) A. Bakač, T. D. Hand, and A. G. Sykes, *Inorg. Chem.*, **14**, 2540 (1975).
(14) See paragraph at end of paper regarding supplementary material.
(15) F. A. Armstrong, R. A. Henderson, and A. G. Sykes, to be published.
(16) M. Goldberg and I. Pecht, *Biochemistry*, **15**, 4197 (1976).
(17) M. G. Segal and A. G. Sykes, *J. Am. Chem. Soc.*, **100**, 4585 (1978).
(18) A. G. Lappin, M. G. Segal, D. C. Weatherburn, and A. G. Sykes, *J. Am. Chem. Soc.*, **101**, 2297, 2302 (1979).
(19) K. T. Yasunobu and M. Tanaka, "Iron-Sulphur Proteins," Vol. II, W. Lovenberg, Ed., Academic Press, New York, 1973, Chapter 2.
(20) K. N. Raymond, D. W. Meek, and J. A. Ibers, *Inorg. Chem.*, 7, 1111 (1968).
(21) D. W. Meek and J. A. Ibers, *Inorg. Chem.*, **9**, 465 (1970).
(22) N. Tanaka and A. Yamada, *Fresenius' Z. Anal. Chem.*, **224**, 117 (1967).
(23) R. A. Henderson and A. G. Sykes, to be published.
(24) L. Hin-Fat and W. C. E. Higginson, *J. Chem. Soc. A*, 298 (1967).

Unusual Structural and Reactivity Types for Copper(I). Synthesis and Structural and Redox Properties of Binuclear Copper(I) Complexes Which Are Probably Three Coordinate in Solution and Experience Intermolecular Metal–Metal Interactions in the Solid State

Robert R. Gagné,* Robert P. Kreh, and John A. Dodge

Contribution No. 5645 from the Division of Chemistry and Chemical Engineering, California Institute of Technology, Pasadena, California 91125.

Received April 4, 1979

Abstract: Condensation of 2-hydroxy-5-methylisophthalaldehyde with 2-(2′-aminoethyl)pyridine, followed by addition of $Cu(CH_3CN)_4BF_4$ and pyrazolate, resulted in formation of a binuclear copper(I) complex, Cu^I_2ISOIM(Etpy)$_2$(pz). A complete crystal and molecular structural analysis showed each Cu(I) to be bound to the phenoxide oxygen as well as to one imine and one pyrazolate nitrogen. In addition each Cu(I) apparently experiences intermolecular copper–copper interactions, with an intermolecular Cu–Cu separation of 2.97 Å. The pyridine was found to be not coordinated to copper. Overall coordination about copper(I) is best described as highly distorted pyramidal, with long axial coordination. In the solid state Cu^I_2ISOIM(Etpy)$_2$(pz) exhibits an electronic absorption spectral band at 600 nm, which is not found in solution spectra, and which is attributed to the copper–copper interaction. Analogous Cu^ICu^I complexes were also prepared using a variety of amines instead of 2-(2′-aminoethyl)pyridine as side arms, and the 3,5-dimethylpyrazole or 7-azaindole anions as bridging groups. Amines without coordinating substituents also gave stable complexes; e.g., *tert*-butylamine gave Cu^I_2ISOIM(*t*-Bu)$_2$(pz). The latter complex did not exhibit an absorption at 600 nm in the solid state or in solution. It appears likely that Cu^I_2ISOIM(*t*-Bu)$_2$(pz) contains three-coordinate Cu(I) both in the solid state and in solution. Moreover, all Cu^ICu^I complexes examined may involve only three-coordinate Cu(I) in solution, yet they have exhibited no tendency to bind additional ligands, such as CO or pyridine. Most of the binuclear copper(I) complexes gave quasi-reversible electrochemical behavior, with two distinct, one-electron redox processes. The most positive reduction potentials obtained were $E_1^f = +0.239$, $E_2^f = +0.080$ V vs. NHE. Biological implications of the observed reactivities and redox properties of the new complexes are discussed.

Introduction

Protein binuclear copper sites effect remarkable reactions with dioxygen including reversible binding (hemocyanin),[1] activation (tyrosinase),[2] and reduction (laccase).[3] Structural information contrasting these active sites is limited but similarities are notable: sulfur ligands have been proposed but most studies suggest only nitrogen and/or oxygen coordination;[4] in the oxidized forms all three binuclear sites are strongly antiferromagnetically coupled;[5,6] the tyrosinase and laccase binuclear sites exhibit two-electron reductions at potentials which are rather high for the proposed all nitrogen/oxygen copper coordination.[6,7]

Model studies have addressed ligand environment(s), redox properties, magnetic interactions, and dioxygen binding in these protein active sites.[8-12] To help define protein structure/reactivity relationships we are endeavoring to catalog fundamental copper(I) coordination chemistry in relatively simple mononuclear and binuclear complexes. As discussed elsewhere, polydentate ligands, including macrocycles, can be utilized to minimize problems associated with both copper(II) and copper(I) substitution lability.[13,14] This approach has

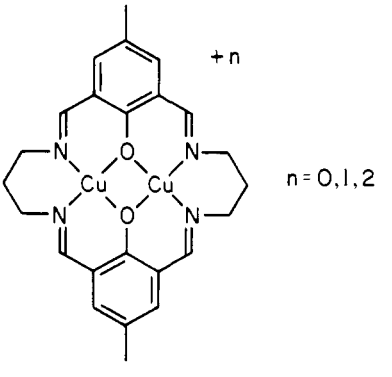

I

0002-7863/79/1501-6917$01.00/0

Table I. Binuclear $Cu^{I}Cu^{I}$ Complexes, Abbreviations Utilized, and NMR Data

compd no.	side arm (R)	bridge (X)	abbreviation	NMR assignments[a] α_1	α_2	α_3	β_1	β_2	py_1	pz_2	pz_3	aza_2	aza_3	aza_6
6	2-(pyridyl)-methyl	pyrazolate	$Cu^{I}_2ISOIM(Mepy)_2(pz)$	2.05	6.66	7.56	4.60		8.46	8.02	6.23			
7	2-(pyridyl)-methyl	3,5-dimethyl-pyrazolate	$Cu^{I}_2ISOIM(Mepy)_2(Me_2pz)$	2.06, s	6.69, s	7.72, s	4.67, s		8.37, d	2.13, s[b]	6.21			
8	2-(pyridyl)-methyl	7-azaindolate	$Cu^{I}_2ISOIM(Mepy)_2$ (az-a)	2.09, s	6.72	7.54	4.70, s		8.43, d			c	c	c
9	2-(2′-pyridyl)-ethyl	pyrazolate	$Cu^{I}_2ISOIM(Etpy)_2(pz)$	1.92, s	6.47	7.50	3.82, t	3.29, t	8.42, d	7.87	6.47			
10	2-(2′-pyridyl)-ethyl	3,5-dimethyl-pyrazolate	$Cu^{I}_2ISOIM(Etpy)_2(Me_2pz)$	1.94, s	6.48, s	7.52, s	3.88, t	3.37, t	8.40, d	2.46, s[b]	6.17			
11	2-(2′-pyridyl)-ethyl	7-azaindolate	$Cu^{I}_2ISOIM(Etpy)_2(aza)$	1.96, s	c	7.60	3.90, t	3.44, 3.20	8.39			8.10	c	8.39
12	phenylmethyl	pyrazolate	$Cu^{I}_2ISOIM(MePh)_2(pz)$	2.10, s	6.72	7.54	4.26			8.00	6.26			
13	phenylmethyl	3,5-dimethyl-pyrazolate	$Cu^{I}_2ISOIM(MePh)_2(Me_2pz)$	2.10, s	6.70	7.57	4.37			2.06, s[b]	c			
14	phenylmethyl	7-azaindolate	$Cu^{I}_2ISOIM(MePh)_2$ (az-a)	2.14, s	6.77	c	4.40, 4.32					c	c	c
15	2-phenylethyl	pyrazolate	$Cu^{I}_2ISOIM(EtPh)_2(pz)$	1.96, s	6.51	7.37	3.45, t	3.07, t		7.93, d	6.51			
16	2-phenylethyl	3,5-dimethyl-pyrazolate	$Cu^{I}_2ISOIM(EtPh)_2(Me_2pz)$	1.97, s	6.52, s	7.38, s	3.50, t	3.10, t		2.61, s[b]	6.17			
17	2-phenylethyl	7-azaindolate	$Cu^{I}_2ISOIM(EtPh)_2(aza)$	1.98, s	6.53, s	7.46, s	3.52, t	3.18, 2.97				8.13, d	c	8.36, d
18	*n*-propyl	pyrazolate	$Cu^{I}_2ISOIM(1\text{-}Pr)_2(pz)$	2.09, s	6.70, s	7.57, s	3.15, t	1.78, m		7.87, d	6.43, t			
19	isopropyl	pyrazolate	$Cu^{I}_2ISOIM(2\text{-}Pr)_2(pz)$	2.10, s	6.70, s	7.70, s	2.90, m	1.20, d		7.87, d	6.45, t			
20	*tert*-butyl	pyrazolate	$Cu^{I}_2ISOIM(t\text{-}Bu)_2(pz)$	2.13, s	6.85, s	7.91, s		1.26, s		7.93, d	6.54, t			
21	*tert*-butyl	3,5-dimethyl-pyrazolate	$Cu^{I}_2ISOIM(t\text{-}Bu)_2(Me_2pz)$	2.10, s	6.81, s	7.85, s		1.28, s		2.57, s[b]	6.10, s			
22	*tert*-butyl	7-azaindolate	$Cu^{I}_2ISOIM(t\text{-}Bu)_2(aza)$	2.14, s	6.85, s	7.98, s		1.34, s 1.23, s				8.13, d	6.75, d	8.45, d
23	phenyl	pyrazolate	$Cu^{I}_2ISOIM(Ph)_2(pz)$	2.04, s	6.67	7.52				7.75, d	6.33			
24	*p*-(dimethyl-amino)-phenyl	pyrazolate	$Cu^{I}_2ISOIM(PhNMe_2)_2(pz)$	2.07	c	7.55				c	c			
25	*p*-acetylphenyl	pyrazolate	$Cu^{I}_2ISOIM(PhCOMe)_2(pz)$	c	c	c				c	c			

[a] All spectra were obtained in benzene-d_6 solution at 34 °C. The values listed are given in parts per million, δ, relative to Me_4Si. The assignments for the resonances are given in Figure 2 and as follows: α_1 = protons from the methyl group on the aromatic ring arising from 2-hydroxy-5-methylisophthalaldehyde; α_2 = aromatic protons from the 2-hydroxy-5-methylisophthalaldehyde ring; α_3 = the imine protons; β_1 = methylene protons (or methine proton) adjacent to the imine nitrogen; β_2 = methylene (or methyl) protons two carbons away from the imine nitrogen; py_1 = the protons on the carbon adjacent to the pyridine nitrogen; pz_2 = protons in the 2 and 4 positions on the pyrazole ring; pz_3 = proton in the 3 position on the pyrazole ring; aza_2, aza_3, aza_6 = the protons on the 2, 3, and 6 positions, respectively, on the 7-azaindole bridge. s = singlet, d = doublet, t = triplet, m = multiplet. If not listed in the table, the multiplicity could not be determined owing to broadness or overlapping of the peaks. [b] These peaks are assigned to the methyl groups attached to the pyrazole ring. [c] These peaks could not be discerned because of overlapping peaks and/or limited solubility.

resulted in unusual structural and reactivity types for copper including four- and five-coordinate copper(I) species.[13-15] The binuclear complex **1** provided an opportunity for measuring intramolecular electron transfer rates between copper centers, but the reduction potentials observed for **1** (eq 1 and 2) are significantly more negative than those exhibited by the proteins (e.g., +0.36 V for tyrosinase).[7,14]

$$Cu^{II}Cu^{II}L^{2+} + e^- \overset{-0.52\ V}{\rightleftharpoons} Cu^{II}Cu^{I}L^{+} \quad (1)$$

$$Cu^{II}Cu^{I}L^{+} + e^- \overset{-0.91\ V}{\rightleftharpoons} Cu^{I}Cu^{I}L \quad (2)$$

Modification of the macrocyclic complex, **1**, has yielded a series of binuclear complexes **2**, in which the R and X groups

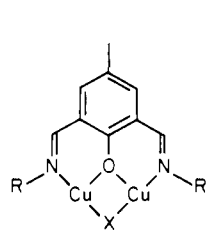

2

X =

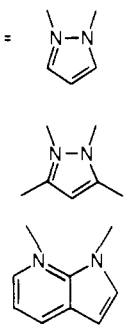

were varied systematically, resulting in wide range of reduction potentials. In this manner, utilizing only nitrogen and oxygen ligands, high reduction potentials comparable to that of protein binuclear sites have been achieved. The new binuclear copper(I) complexes appear to be only three coordinate in solution but in some instances experience significant intermolecular copper(I)–copper(I) interactions in solid state.

Synthesis and Characterization of Complexes

Three copper(II) complexes, **3–5**, were prepared by simple condensation of 2-hydroxy-5-methylisophthalaldehyde with primary amines followed by addition of copper(II), Scheme I. The new compounds are blue-green owing to weak absorption in the 630–645-nm region (probably ligand field transitions) as listed in Scheme I for methanol solutions. Solid-state magnetic susceptibility measurements at 25 °C, also listed in Scheme I, suggest that the two copper(II) centers are antiferromagnetically coupled.

Analogous air-sensitive copper(I) complexes were prepared in a helium atmosphere in a fashion similar to the synthesis of the copper(II) species. The dialdehyde was condensed with 2 equiv of a primary amine, RNH_2, then treated with a bridging bidentate ligand, XH, in the presence of base, followed by addition of $Cu(CH_3CN)_4BF_4$ (Scheme II). The compounds synthesized, along with the abbreviations to be used, are listed in Table I. All of the compounds listed gave satisfactory C, H, and N analyses. Selected compounds were also analyzed for

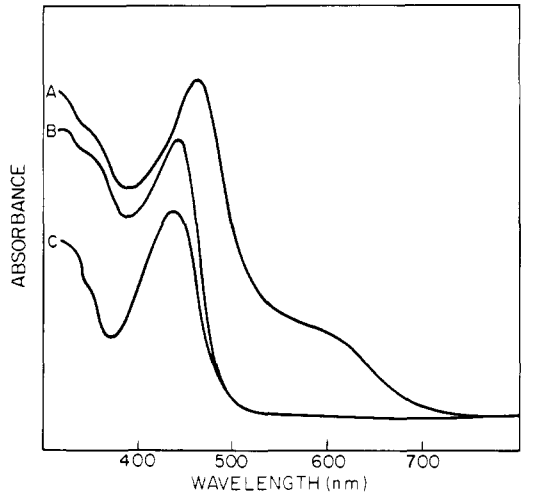

Figure 1. Electronic absorption spectra: (A) Cu^{I}_2ISOIM(EtPh)$_2$(pz) (**15**) in the solid state; (B) Cu^{I}_2ISOIM(EtPh)$_2$(pz) (**15**) in a hexane solution; (C) Cu^{I}_2ISOIM(*t*-Bu)$_2$(pz) (**20**) in the solid state.

Scheme I. Preparation of Binuclear $Cu^{II}Cu^{II}$ Complexes[a]

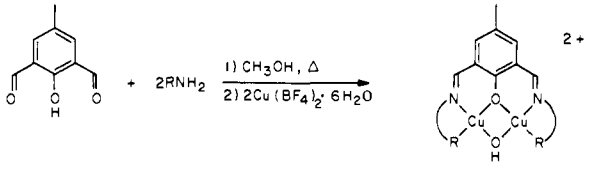

	R	λ (ε)	μ_{eff}/Cu
3	$-CH_2-$ 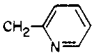	630 (160)	1.4
4	$-CH_2CH_2-$ 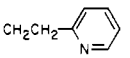	645 (120)	1.2
5	$-CH_2CH_2-$ 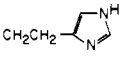	630 (100)	0.96

[a] Spectra were recorded in methanol solution at 25 °C. Magnetic susceptibilities are given in Bohr magnetons, measured at 25 °C, and corrected for diamagnetism but not for TIP.

copper, giving the expected values. The infrared spectra of all compounds showed the absence of aldehydic carbonyl and amine N–H stretches, consistent with complete imine condensation. The multitude of peaks in the region 700–1640 cm^{-1} made absolute assignments difficult.

Mass spectra were obtained for compounds **16, 19, 20, 21,** and **22,** each of which exhibits parent ion peaks in agreement with the formulation given above. The presence of two coppers in these compounds is indicated by three parent peaks due to the presence of both ^{63}Cu and ^{65}Cu. The relative intensities of these three peaks, averaged over all the compounds analyzed, were 1:0.90:0.24 for $^{63}Cu_2L$:$^{63}Cu^{65}CuL$:$^{65}Cu_2L$ (theoretical ratio is 1:0.89:0.20).

The electronic absorption spectrum of Cu^{I}_2ISOIM(EtPh)$_2$(pz) (**15**), shown in Figure 1 (curve B), is typical of the solution spectrum of all the binuclear copper(I) complexes examined. Spectra obtained in the solid state (Nujol mulls) varied. The solid-state spectrum of Cu^{I}_2ISOIM(EtPh)$_2$(pz) (**15**), shown in Figure 1 (curve A), is typical of that for most compounds examined. Note that the absorption present in solution at 444 nm (ϵ 8600) shifts to lower energies, ca. 464 nm, in the solid state. In addition a new absorption was found in the solid-state spectrum at ca. 600 nm. The 600-nm absorption was not found in solution even in spectra of concentrated THF

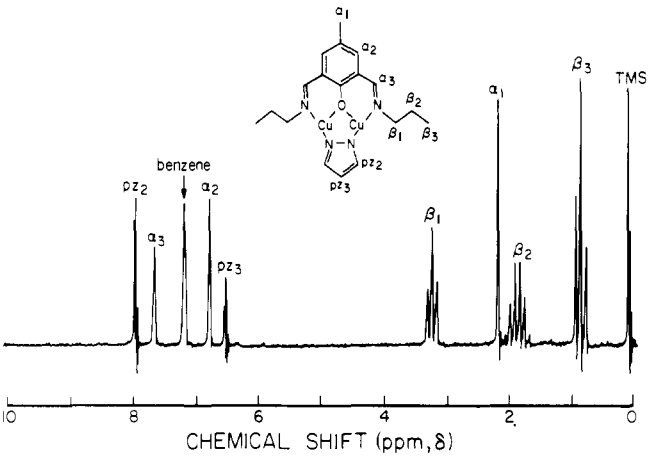

Figure 2. NMR spectrum of Cu^{I}_2ISOIM(1-Pr)$_2$(pz) (**18**) in benzene-d_6 at 34 °C.

Scheme II

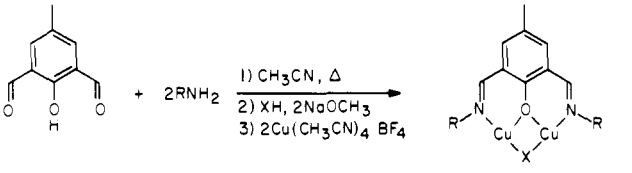

solutions, in which these compounds are considerably soluble.

Not all species examined exhibit the solid-state spectrum described above. Compounds **19–22** exhibit solid-state spectra as shown for Cu^{I}_2ISOIM(*t*-Bu)$_2$(pz) (**20**) in Figure 1 (curve C), which can be compared to the solution spectra of all complexes. Under no conditions have compounds **19–22** shown notable absorption in the 600-nm region.

All cuprous compounds were shown to be diamagnetic by the presence of very sharp NMR resonances (see Figure 2). Table I lists the peaks observed for each complex. The assignments given were made by cross comparisons of all the spectra. In each case, the identity of the organic entity is confirmed. Integration values were in agreement with the proposed structures.

Solution Reactivity. All compounds presented here are unreactive toward carbon monoxide. This was shown definitively for CO-saturated solutions (CH_2Cl_2) of Cu^{I}_2ISOIM(Etpy)$_2$(pz) (**9**) and Cu^{I}_2ISOIM(1-Pr)$_2$(pz) (**18**) both of which show infrared absorptions in the region 1500–1650 cm^{-1}, characteristic of the original complex, **9** or **18,** but neither shows any bands in the region 1700–2200 cm^{-1} which would be attributable to a carbonyl complex. Also, evaporation of THF solutions of these compounds with a stream of CO gave the original compounds, as identified by IR spectra.

All copper(I) compounds react with oxygen at the ambient temperature to form green or brown products from orange DMF solutions. This reaction could not be reversed by subsequent bubbling of argon through the solutions. The air sensitivity of these complexes prevented reliable solution molecular weight measurements.

Electrochemistry. All electrochemical results presented here were obtained in DMF solutions at a platinum indicating electrode. Ferrocene was used as an internal standard and all potentials have been converted to vs. NHE using E^f = +0.40 mV vs. NHE for ferrocene.[16] The cyclic voltammograms for the Cu(II) compounds, **3–5,** were irreversible as shown in Figure 3 for Cu^{II}_2ISOIM(Mepy)$_2$(OH)$^{2+}$ (**3**). Addition of 1 equiv of pyrazole to the same solution, however, gave the quasi-reversible electrochemistry also shown in Figure 3.[17]

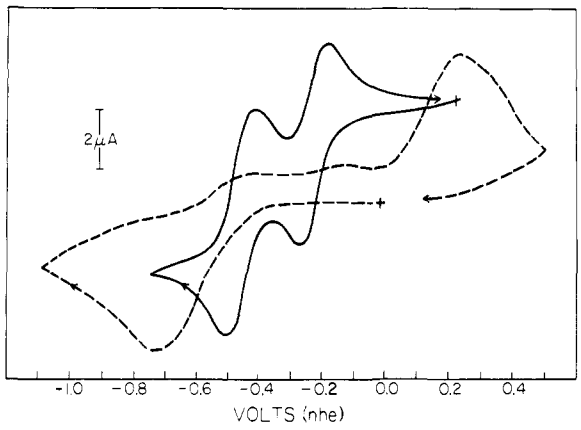

Figure 3. Cyclic voltammograms of DMF solutions: Cu^{II}_2ISOIM-$(Mepy)_2(OH)^{2+}$ (**3**, - - - -); Cu^{II}_2ISOIM$(Mepy)_2(OH)^{2+}$ (**3**, containing 1 equiv of pyrazole, ——). Both voltammograms were observed with a platinum electrode, using 0.1 M TBAP as the electrolyte at a scan rate of 200 mV/s.

Similar results were observed for Cu^{II}_2ISOIM$(Etpy)_2(OH)^{2+}$ (**4**). In contrast Cu^{II}_2ISOIM$(hist)_2(OH)^{2+}$ (**5**) gave very irreversible electrochemistry even with added pyrazole.

Constant-potential electrolysis (CPE) of **3** plus an equivalent amount of pyrazole at −0.35 and −0.70 V indicated that each wave corresponded to a one-electron process. No attempt was made to isolate a mixed valence species, but the binuclear cuprous complex, Cu^{I}_2ISOIM$(Mepy)_2(pz)$ (**6**), was synthesized by CPE of an acetonitrile solution containing Cu^{II}_2ISOIM-$(Mepy)_2(OH)^{2+}$ (**3**) and an equivalent amount of pyrazole at −0.70 V (n = 2.0).

The cyclic voltammogram for Cu^{I}_2ISOIM$(Mepy)_2(pz)$ (**6**) was, of course, identical with that shown in Figure 3 for **3** plus 1 equiv of pyrazole. All binuclear copper(I) compounds presented in Table II exhibited cyclic voltammetry similar to the solid line in Figure 3; however, large peak separations ($E_{p_a} - E_{p_c}$ = 100–150 mV at 50 mV/s) were observed for many compounds at a platinum electrode.[18] Cyclic voltammetry at a hanging mercury drop electrode (HMDE) gave smaller peak separations (70–90 mV) for most compounds, and the formal potentials (E^f) were identical with those observed using a platinum electrode. The potentials recorded in Table II were determined at a platinum electrode because this electrode allowed direct comparison with the internal standard, ferrocene, on the same scan. It was found that the potentials could be read more accurately using differential pulse voltammetry and this technique was employed to obtain the values presented in Table II. In all cases, the formal potentials were within 10 mV of the potentials observed by cyclic voltammetry. All compounds containing the 7-azaindole anion as the bridge exhibited irreversible electrochemistry, often showing two anodic waves but only ill-defined cathodic waves, and hence the electrochemistry of these species is not included here.

Constant-potential electrolysis at a potential 200 mV more positive than the second oxidation peak was performed on compounds **6, 9, 10, 19,** and **20,** as typical Cu(I) species, and each gave a two-electron oxidation (n = 2.0 ± 0.1).

The average separation of the two formal potentials ($E_1^f - E_2^f$) is 194 ± 40 mV for all new compounds listed in Table II. From this value for $E_1^f - E_2^f$, the average comproportionation constant, K, is calculated to be 1.9×10^3 for the equilibrium

$$Cu^{I}Cu^{I}L + Cu^{II}Cu^{II}L^{2+} \overset{K}{\rightleftharpoons} 2Cu^{II}Cu^{I}L^{+} \qquad (3)$$

where L represents the entire ligand system.[14] Note that all complexes containing a 3,5-dimethylpyrazolate bridge have smaller formal potential separations ($E_1^f - E_2^f$) and correspondingly smaller comproportionation constants than their pyrazolate bridged analogues.

Addition of excess pyridine (up to 100-fold excess) to the electrochemical solutions of **6, 12,** and **13** did not cause a significant shift (<10 mV) in the potentials, but merely broadened the peaks. Cyclic voltammetry of **6, 7, 9,** and **10** in other solvents such as CH_2Cl_2, CH_3CN, and THF gave similar behavior to that observed in DMF, while the electrochemistry for all other compounds was irreversible in these alternative solvents.

Table II. Reduction Potentials for Binuclear Copper Complexes[a]

$$Cu^{II}Cu^{II}L^{2+} + e^- \overset{E_1^f}{\rightleftharpoons} Cu^{II}Cu^{I}L^{+}$$

$$Cu^{II}Cu^{I}L^{2+} + e^- \overset{E_2^f}{\rightleftharpoons} Cu^{I}Cu^{I}L$$

no.	compd	E_1^f [b]	E_2^f [b]	n[c]
1	Cu^{II}_2(ISOIM)$_2(Pr)_2^{2+}$	−0.52[d]	−0.91[d]	
6	Cu^{I}_2ISOIM$(Mepy)_2(pz)$	−0.211	−0.452	2.0
7	Cu^{I}_2ISOIM$(Mepy)_2(Me_2pz)$	−0.190	−0.374	
9	Cu^{I}_2ISOIM$(Etpy)_2(pz)$	−0.110	−0.344	2.0
10	Cu^{I}_2ISOIM$(Etpy)_2(Me_2pz)$	−0.113	−0.267	2.0
12	Cu^{I}_2ISOIM$(MePh)_2(pz)$	0.146	−0.081	
13	Cu^{I}_2ISOIM$(MePh)_2(Me_2pz)$	0.206	0.005	
15	Cu^{I}_2ISOIM$(EtPh)_2(pz)$	0.128	−0.078	
16	Cu^{I}_2ISOIM$(EtPh)_2(Me_2pz)$	0.205	0.009	
18	Cu^{I}_2ISOIM$(1\text{-}Pr)_2(pz)$	0.146	−0.076	
19	Cu^{I}_2ISOIM$(2\text{-}Pr)_2(pz)$	0.193	0.001	1.9
20	Cu^{I}_2ISOIM$(t\text{-}Bu)_2(pz)$	0.240	0.053	2.0
21	Cu^{I}_2ISOIM$(t\text{-}Bu)_2(Me_2pz)$	0.239	0.080	
23	Cu^{I}_2ISOIM$(Ph)_2(pz)$	0.144	−0.032	
24	Cu^{I}_2ISOIM$(PhNMe_2)_2(pz)$	0.146	−0.048	
25	Cu^{I}_2ISOIM$(PhCOMe)_2(pz)$	0.152	0.008	

[a] These values were measured by differential pulse voltammetry in DMF using a platinum indicating electrode. [b] Potentials are given in volts vs. NHE. Potentials were measured vs. ferrocene as an internal redox couple, then corrected to vs. NHE using a value of 0.40 V for ferrocene vs. NHE. [c] These values for n were determined by constant-potential electrolysis at a potential 200 mV more positive than E_1^f. Values are given for all complexes actually examined by CPE. [d] Reference 13.

Table III. Basic Crystal Data for Cu^{I}_2ISOIM$(Etpy)_2(pz)$ (**9**)

$C_{26}H_{26}Cu_2N_6O$	
mol wt = 565.6	V = 2502.3 (10) Å^3
space group $P2_1/c$ (no. 14)	Z = 4
a = 20.980 (4) Å	ρ_{calcd} = 1.50 g cm^{-3}
b = 4.929 (1) Å	μ = 23.8 cm^{-1}
c = 24.773 (6) Å	λ(Cu Kα) = 1.5418 Å
β = 102.38 (2)°	

Crystallographic Analysis

The crystal and molecular structure of Cu^{I}_2ISOIM$(Etpy)_2(pz)$ (**9**) was determined. Basic crystal data are summarized in Table III. Tables IV–VII present the atomic parameters and interatomic distances and angles. The atom labeling scheme is illustrated in Figure 4.

The bonds to the copper atoms are shown in Figure 4. Each copper is bound to three ligand atoms in what is almost a tee geometry, the largest angles being 167.6 (N1–Cu1–N3) and 170.7° (N2–Cu2–N4). The intramolecular copper–copper distance, 3.304 Å, is sufficiently long that any direct interaction is unlikely.

There still remains, however, the possibility of direct *intermolecular* interaction between copper atoms. The molecules form an infinite stack in the direction of the b axis, a section

Table IV. Atomic Parameters and esd's for Cu^{I}_2ISOIM(Etpy)$_2$(pz) (**9**)

	x^a	y	z	$U_{11}{}^b$	U_{22}	U_{33}	U_{12}	U_{13}	U_{23}
Cu1	23 717 (3)	124 543 (14)	37 118 (3)	535 (4)	554 (4)	607 (4)	−53 (4)	112 (3)	54 (4)
Cu2	18 840 (3)	70 218 (13)	42 920 (3)	492 (4)	575 (4)	585 (4)	−82 (4)	117 (3)	26 (4)
O1	2624 (1)	99 60 (6)	4407 (1)	51 (2)	46 (2)	51 (2)	−8 (2)	8 (1)	6 (2)
N1	3176 (2)	14 363 (7)	3905 (1)	56 (2)	45 (2)	50 (2)	−7 (2)	18 (2)	2 (2)
N2	2229 (2)	5481 (7)	4994 (1)	51 (2)	41 (2)	58 (2)	−4 (2)	23 (2)	3 (2)
N3	1614 (2)	10 565 (8)	3366 (2)	57 (2)	58 (3)	63 (3)	−3 (2)	4 (2)	9 (2)
N4	1412 (2)	8318 (7)	3610 (1)	51 (2)	55 (3)	62 (2)	−3 (2)	7 (2)	1 (2)
N5	4090 (2)	18 214 (9)	2575 (2)	89 (3)	79 (3)	64 (3)	−4 (3)	27 (2)	−5 (3)
N6	1383 (2)	1473 (10)	6244 (2)	94 (3)	90 (4)	83 (3)	−7 (3)	31 (3)	5 (3)
C1	3161 (2)	10 007 (8)	4783 (2)	48 (2)	41 (3)	49 (3)	−1 (2)	14 (2)	−6 (2)
C2	3667 (2)	11 901 (8)	4760 (2)	47 (2)	44 (3)	50 (2)	−4 (2)	16 (2)	−3 (2)
C3	3633 (2)	13 920 (9)	4330 (2)	54 (3)	46 (3)	57 (3)	−9 (2)	22 (2)	−10 (2)
C4	4231 (2)	11 854 (9)	5181 (2)	45 (2)	54 (3)	65 (3)	−4 (2)	16 (2)	−6 (3)
C5	4326 (2)	10 099 (10)	5624 (2)	45 (2)	65 (3)	54 (3)	−1 (2)	10 (2)	−7 (3)
C6	4942 (3)	10 164 (16)	6072 (3)	55 (3)	113 (5)	78 (4)	−5 (3)	−2 (3)	4 (4)
C7	3833 (2)	8315 (10)	5645 (2)	54 (3)	61 (3)	48 (3)	1 (2)	15 (2)	1 (2)
C8	3249 (2)	8178 (8)	5237 (2)	45 (2)	47 (3)	46 (2)	−5 (2)	13 (2)	−3 (2)
C9	2784 (2)	6107 (9)	5313 (2)	57 (3)	54 (3)	49 (3)	3 (2)	20 (2)	5 (2)
C10	868 (2)	7395 (12)	3265 (2)	58 (3)	74 (4)	74 (3)	−13 (3)	5 (3)	−4 (3)
C11	719 (3)	8962 (12)	2806 (2)	61 (3)	90 (4)	66 (3)	1 (3)	−7 (3)	−6 (3)
C12	1187 (3)	10 881 (11)	2876 (2)	76 (3)	67 (4)	67 (3)	2 (3)	0 (3)	6 (3)
C13	3289 (3)	16 574 (9)	3531 (2)	73 (3)	44 (3)	57 (3)	−8 (2)	22 (2)	0 (2)
C14	3398 (3)	15 393 (11)	2997 (2)	124 (5)	56 (3)	76 (4)	−9 (3)	47 (3)	2 (3)
C15	3480 (2)	17 556 (10)	2591 (2)	86 (3)	55 (3)	51 (3)	−9 (3)	23 (3)	−6 (3)
C16	2955 (3)	18 762 (13)	2257 (2)	83 (4)	85 (4)	72 (4)	−11 (3)	22 (3)	−14 (3)
C17	3054 (3)	20 797 (13)	1894 (2)	114 (5)	87 (4)	53 (3)	16 (4)	2 (3)	−5 (3)
C18	3670 (4)	21 466 (12)	1877 (2)	148 (6)	72 (4)	60 (3)	−7 (4)	43 (4)	0 (3)
C19	4166 (3)	20 198 (13)	2217 (3)	92 (4)	85 (4)	80 (4)	−20 (4)	37 (3)	−8 (4)
C20	1866 (2)	3367 (9)	5219 (2)	56 (3)	50 (3)	62 (3)	−9 (2)	22 (2)	4 (2)
C21	1377 (3)	4646 (11)	5507 (3)	71 (3)	63 (3)	99 (4)	6 (3)	45 (3)	7 (3)
C22	1030 (2)	2604 (10)	5789 (2)	60 (3)	62 (3)	75 (3)	−7 (3)	35 (3)	−5 (3)
C23	392 (3)	2021 (13)	5593 (2)	63 (3)	106 (5)	87 (4)	−4 (4)	27 (3)	0 (4)
C24	98 (3)	119 (17)	5871 (3)	77 (4)	147 (7)	131 (6)	−45 (5)	46 (4)	−36 (6)
C25	443 (4)	−1058 (15)	6319 (3)	136 (6)	114 (6)	119 (6)	−39 (5)	85 (5)	−11 (5)
C26	1070 (4)	−366 (14)	6499 (3)	145 (6)	94 (5)	77 (4)	0 (5)	44 (4)	14 (4)

	x	y	z	B, Å^2		x	y	z	B, Å^2
H3	401 (2)	1530 (8)	438 (2)	5.00	H14′	378 (2)	1416 (10)	310 (2)	7.20
H4	451 (2)	1324 (8)	517 (2)	5.10	H16	256 (2)	1839 (9)	228 (2)	7.00
H6	502 (2)	1180 (10)	623 (2)	8.00	H17	268 (2)	2170 (9)	166 (2)	7.70
H16	529 (2)	1008 (11)	595 (2)	8.00	H18	376 (2)	2302 (9)	166 (2)	7.30
H6	495 (2)	864 (10)	628 (2)	8.00	H19	460 (2)	2057 (9)	224 (2)	7.40
H7	385 (2)	693 (8)	592 (2)	5.00	H20	215 (2)	213 (8)	548 (2)	5.30
H9	291 (2)	506 (8)	565 (2)	5.10	H20′	164 (2)	216 (8)	493 (2)	5.30
H10	69 (2)	577 (9)	338 (2)	6.10	H21	108 (2)	554 (9)	522 (2)	6.30
H11	38 (2)	879 (9)	253 (2)	6.60	H21′	156 (2)	587 (9)	577 (2)	6.30
H12	125 (2)	1252 (9)	268 (2)	6.70	H23	15 (2)	295 (9)	527 (2)	7.00
H13	362 (2)	1758 (8)	371 (2)	5.40	H24	−36 (2)	−46 (10)	573 (2)	9.10
H13′	288 (2)	1786 (8)	346 (2)	5.40	H25	25 (2)	−242 (10)	652 (2)	8.50
H14	298 (2)	1442 (10)	283 (2)	7.20	H26	135 (2)	−113 (10)	682 (2)	9.10

[a] Fractional coordinates have been multiplied by factors of 10^5 for the copper atoms, 10^4 for the remaining nonhydrogen atoms, and 10^3 for the hydrogen atoms. U_{ij} has been multiplied by 10^4 for the copper atoms and 10^3 for the remaining nonhydrogen atoms. [b] The form of the thermal ellipsoid is $\exp[-2\pi^2(U_{11}h^2a^{*2} + \cdots + 2U_{23}klb^*c^*)]$ for the anisotropic thermal parameters.

of which is shown in Figure 5. Although the separation between molecules in the direction of the *b* axis is 4.929 Å (just the length of the *b* axis), the molecule is far from perpendicular to this axis, the angle between the axis and the mean molecular plane being 41°. Thus, "overlapping" portions of neighboring molecules come rather close to one another. The average distance of atoms O1, C1, C8, C9, and N2 from the mean plane of atoms N1, C3, C2, C1, and O1 in the neighboring molecule just below is 3.20 Å. This is somewhat shorter than the separation usually observed between stacked π-delocalized molecules.[19] The intermolecular copper–copper distance is shorter yet, at 2.968 Å.

A least-squares plane calculation including the atoms of the benzene ring, the methyl carbon, and the phenolic oxygen shows these atoms to be coplanar, with no deviation from the mean plane exceeding 0.009 Å. The deviations of the copper atoms from this plane are 0.04 Å for Cu1 and 0.29 Å for Cu2. In each case the direction of the out-of-plane separation is that which reduces the *intermolecular* copper–copper distance. Each of the two C=N groups is also twisted slightly out of plane in the direction of the copper atom to which it is bound (deviations: 0.04 Å for C3, 0.05 Å for N1, 0.04 Å for C9, and 0.10 Å for N2).

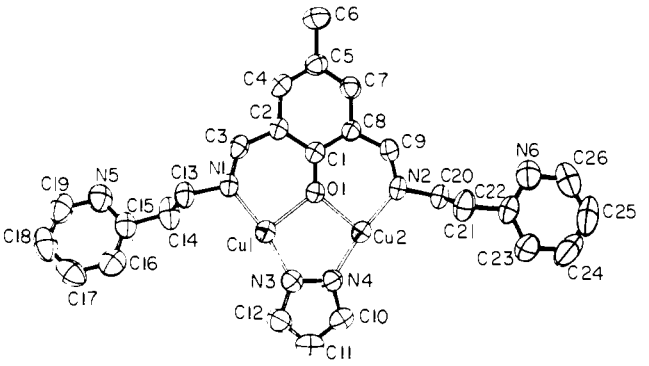

Figure 4. ORTEP drawing of Cu^{I}_2ISOIM(Etpy)$_2$(pz) (**9**), including atomic labeling scheme. Each hydrogen is given the same number as the carbon to which it is bound.

The atoms of the pyrazolate group are coplanar with no deviation from the mean plane exceeding 0.006 Å. The benzene and pyrazole rings are not quite coplanar, the dihedral angle being 170 (3)°.

There is also a slight deviation of each copper atom from the plane defined by the three atoms to which it is bound. These

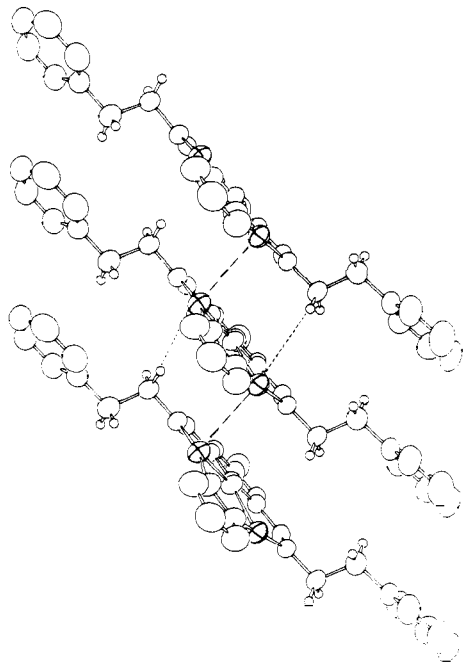

Figure 5. Crystal packing of Cu^{I}_2ISOIM(Etpy)$_2$(pz) (**9**) showing a section of an infinite stack of molecules which forms in the solid state. The three molecules are corresponding ones from three different unit cells, translated along the *b* axis (which lies in the vertical direction in the orientation of this figure). All copper atoms lie in the same plane, parallel to the page. The pyrazolate groups are directed out of the page, toward the reader. The shortest copper–copper distance, 2.97 Å, occurs between atoms in neighboring molecules, connected by dashed lines in the figure. The two dotted lines correspond to two different intermolecular Cu–H distances, 2.64 (Cu1–H13′) and 3.09 Å (Cu2–H20′).

Table V. Bond Distances (Å) for Cu^{I}_2ISOIM(Etpy)$_2$(pz) (**9**)

Cu1–O1	2.089 (2)	C16–C17	1.391 (8)
Cu1–N1	1.901 (3)	C17–C18	1.344 (8)
Cu1–N3	1.882 (3)	C18–C19	1.345 (9)
Cu2–O1	2.097 (2)	C20–C21	1.508 (7)
Cu2–N2	1.894 (3)	C21–C22	1.499 (7)
Cu2–N4	1.878 (3)	C22–C23	1.354 (7)
O1–C1	1.300 (4)	C23–C24	1.385 (9)
N1–C3	1.281 (5)	C24–C25	1.322 (11)
N1–C13	1.482 (5)	C25–C26	1.339 (10)
N2–C9	1.296 (5)	C3–H3	1.03 (4)
N2–C20	1.469 (5)	C4–H4	0.90 (4)
N3–N4	1.372 (5)	C6–H6	0.90 (5)
N3–C12	1.355 (6)	C6–H6′	0.85 (5)
N4–C10	1.349 (6)	C6–H6″	0.90 (5)
N5–C15	1.330 (6)	C7–H7	0.96 (4)
N5–C19	1.353 (7)	C9–H9	0.96 (4)
N6–C22	1.331 (6)	C10–H10	0.95 (4)
N6–C26	1.354 (8)	C11–H11	0.88 (4)
C1–C2	1.424 (5)	C12–H12	0.96 (4)
C1–C8	1.421 (5)	C13–H13	0.89 (4)
C2–C3	1.449 (5)	C13–H13′	1.05 (4)
C2–C4	1.399 (5)	C14–H14	1.01 (5)
C4–C5	1.378 (6)	C14–H14	0.99 (5)
C5–C6	1.513 (7)	C16–H16	0.87 (4)
C5–C7	1.366 (6)	C17–H17	0.98 (5)
C7–C8	1.413 (5)	C18–H18	0.98 (4)
C8–C9	1.453 (6)	C19–H19	0.91 (5)
C10–C11	1.355 (7)	C20–H20	0.99 (4)
C11–C12	1.348 (7)	C20–H20′	0.97 (4)
C13–C14	1.507 (7)	C21–H21	0.95 (4)
C14–C15	1.501 (7)	C21–H21′	0.90 (4)
C15–C16	1.363 (7)	C23–H23	0.97 (4)
		C24–H24	0.99 (5)
		C25–H25	0.97 (5)
		C26–H26	0.96 (5)

deviations are 0.14 Å for Cu1 and 0.06 Å for Cu2. Again, in each case the direction of the out-of-plane separation is that which reduces the intermolecular copper–copper distance.

It should be noted that a possible attraction for another copper atom is not the only factor favoring this direction for the out-of-plane separation. As shown in Figure 5, there is a hydrogen atom on the opposite side of each copper atom, and in the case of Cu1 this hydrogen is at a distance of 2.64 Å. (This is also the copper that is farther out of its donor-atom plane.) Thus, at least for Cu1, copper–hydrogen steric interactions may influence the out-of-plane displacement of the copper ion.

A final point which should be noted concerning the coordination about copper is that the copper–nitrogen bonds are shorter than most which have been reported for Cu(I) complexes with nitrogen donor ligands.[22] The average lengths are 1.88 Å for the copper–pyrazole nitrogen bonds and 1.90 Å for the copper–imine nitrogen bonds. The copper–oxygen distances are substantially longer than this, averaging 2.09 Å. Also, as stated previously, the N–Cu–N bond angles approach 180° (167.6 and 170.7°). These factors may suggest some degree of two-coordinate character, which may be related to the unusual chemical behavior of the compound (e.g., unreactivity toward CO).

Discussion

The rather negative reduction potentials observed for complex **1** (eq 1 and 2) likely result from a square-planar arrangement of "hard" oxygen and nitrogen ligands.[25] The complexes reported here were designed to stabilize copper(I) in an attempt to better model binuclear copper protein sites. For example, the condensation of 2-hydroxy-5-methylisophthalaldehyde with 2-aminomethylpyridine resulted in the binucleating ligand in **3**, which is more flexible than the ligand system in **1** and also presents relatively soft pyridines for coordination. Two additional binucleating ligands, providing even greater flexibility, were obtained using 2-(2′-aminoethyl)pyridine and histamine, and these ligands reacted readily with copper(II) salts to yield the binuclear copper(II) complexes **4** and **5**. Complexes similar to **4** and **5** were reported during the course of the present study.[26]

In all three copper(II) complexes, both copper atoms are presumably bound to an aromatic nitrogen. This has been demonstrated by an X-ray structure determination of Cu^{II}_2ISOIM(hist)$_2$(OH)$^{2+}$ (**5**).[27] Each copper(II) is actually five coordinate with one of the copper atoms bound to the oxygen of a water molecule and the other copper bound to the oxygen of the hydroxy bridge of an adjacent molecule.

The electrochemistry of these nonmacrocyclic complexes, **3–5**, is irreversible as shown in Figure 3 for Cu^{II}_2ISOIM(Mepy)$_2$(OH)$^{2+}$ (**3**). This may be a result of the relatively labile hydroxy bridge, which is a poor ligand for copper(I). The introduction of pyrazole did produce reversible electrochemical behavior, also shown in Figure 3, leading to the isolation of a stable binuclear copper(I) complex, Cu^{I}_2ISOIM(Mepy)$_2$(pz) (**6**), by constant-potential electrolysis (n = 2).[17] The reduction potentials observed for Cu^{I}_2ISOIM(Mepy)$_2$(pz) (**6**) (E_1^f = −0.21, E_2^f = −0.45 V) were appreciably more positive than those observed for the macrocyclic complex, **1**, indicating that the binucleating ligand in **6** does indeed provide a better environment for copper(I) relative to copper(II).

The copper(I) compound Cu^{I}_2ISOIM(Mepy)$_2$(pz) (**6**) was also synthesized directly from cuprous starting materials. Similar reactions with 2-aminomethylpyridine or 2-(2′-aminoethyl)pyridine as side arms and with pyrazole, 3,5-dimethylpyrazole, or 7-azaindole as bridging ligands gave complexes **7–11**. The coordination environment around each copper(I) of these complexes was expected to be a tetrahedral arrangement of one oxygen and three nitrogen ligands. The

Table VI. Bond Angles (deg) for Cu^{I}_2ISOIM(Etpy)$_2$(pz) (**9**)

O1-Cu1-N1	91.7 (1)	C4-C5-C6	121.8 (4)
O1-Cu1-N3	97.1 (1)	C4-C5-C7	116.9 (4)
N1-Cu1-N3	167.6 (2)	C6-C5-C7	121.3 (4)
O1-Cu2-N2	91.5 (1)	C5-C7-C8	123.4 (4)
O1-Cu2-N4	96.8 (1)	C1-C8-C7	118.8 (4)
N2-Cu2-N4	170.7 (2)	C1-C8-C9	124.8 (4)
Cu1-O1-Cu2	104.2 (1)	C7-C8-C9	116.4 (4)
Cu1-O1-C1	127.5 (3)	N2-C9-C8	129.0 (4)
Cu2-O1-C1	127.7 (3)	N4-C10-C11	110.6 (5)
Cu1-N1-C3	126.1 (3)	C10-C11-C12	105.2 (5)
Cu1-N1-C13	117.3 (3)	N3-C12-C11	111.0 (5)
C3-N1-C13	116.6 (4)	N1-C13-C14	109.8 (4)
Cu2-N2-C9	125.5 (3)	C13-C14-C15	112.1 (5)
Cu2-N2-C20	120.4 (3)	N5-C15-C14	116.2 (4)
C9-N2-C20	114.1 (4)	N5-C15-C16	122.2 (5)
Cu1-N3-N4	120.6 (3)	C14-C15-C16	121.5 (5)
Cu1-N3-C12	133.1 (3)	C15-C16-C17	119.6 (5)
N4-N3-C12	106.3 (4)	C16-C17-C18	118.4 (6)
Cu2-N4-N3	121.2 (3)	C17-C18-C19	119.1 (6)
Cu2-N4-C10	131.8 (3)	N5-C19-C18	124.3 (6)
N3-N4-C10	107.0 (4)	N2-C20-C21	110.1 (4)
C15-N5-C19	116.4 (4)	C20-C21-C22	112.8 (4)
C22-N6-C26	115.9 (5)	N6-C22-C21	116.0 (4)
O1-C1-C2	121.5 (4)	N6-C22-C23	123.0 (5)
O1-C1-C8	120.2 (4)	C21-C22-C23	121.1 (5)
C2-C1-C8	118.4 (4)	C22-C23-C24	118.4 (6)
C1-C2-C3	124.0 (4)	C23-C24-C25	119.5 (7)
C1-C2-C4	118.6 (4)	C24-C25-C26	119.3 (7)
C3-C2-C4	117.4 (4)	N6-C26-C25	123.8 (7)
N1-C3-C2	129.2 (4)		
C2-C4-C5	124.0 (4)		

Table VII. Nonbonding Distances and Associated Angles for Cu^{I}_2ISOIM(Etpy)$_2$(pz) (**9**)

Cu1-Cu2	3.3036 (4)	Cu1-Cu2[a]	2.9685 (4)
Cu1-H13′[b]	2.64 (4)	Cu2-H20′[a]	3.09 (4)
O1-Cu1-Cu2[a]	95.7 (1)	O1-Cu2-Cu1[b]	105.5 (1)
N1-Cu1-Cu2[a]	83.2 (1)	N2-Cu2-Cu1[b]	92.1 (1)
N3-Cu1-Cu2[a]	104.5 (1)	N4-Cu2-Cu1[b]	89.6 (1)

[a] Translated by one unit cell in positive y direction. [b] Translated by one unit cell in negative y direction.

crystallographic results presented herein for Cu^{I}_2ISOIM(Etpy)$_2$(pz) (**9**) did not yield the expected structure. The side-arm pyridine nitrogen atoms are *not* coordinated. The overall coordination about copper approximates trigonal pyramidal, with a long, axial, copper–copper interaction with Cu(1)–Cu(1) = 2.97 Å. Copper(I)–copper(I) interactions with metal separations as short as 2.45 Å are known but in all previously characterized species having proposed Cu(I)–Cu(I) interactions there is at least one bridging ligand between the two interacting copper atoms.[28] It is reasonable to assume that the structures of the analogous species, **6–11,** are similar to this structure found for Cu^{I}_2ISOIM(Etpy)$_2$(pz) (**9**).

The structure of Cu^{I}_2ISOIM(Etpy)$_2$(pz) (**9**) suggested the synthesis of a series of compounds which had *no* donor atoms on the side arms (R), i.e., complexes **12–25,** Table I. These compounds also proved to be crystalline compounds, stable in the absence of dioxygen. Since the polydentate ligand systems employed provide only three coordination for each copper, these compounds are presumed to be three coordinate in solution.

All compounds which have nonbulky side arms are brown in the solid state, this color being due, in part, to a 600-nm band observed in the solid state Nujol mull spectrum (curve A in Figure 1). This band is not present in the spectrum of the complex with *tert*-butyl side arms, Cu^{I}_2ISOIM(*t*-Bu)$_2$(pz) (**20**), which is red in the solid state as well as in solution (curve C in Figure 1). This 600-nm band may be attributed to the *intermolecular* copper–copper interaction which may be inhibited by the presence of large *tert*-butyl side arms. This copper–copper interaction appears to be only a solid-state phenomenon, since the 600-nm band was not found in solution spectra, even in very concentrated solutions.

This novel dimerization of d^{10} copper(I) centers may be closely related to the dimerization observed for rhodium(I), d^8, isocyanide complexes.[29] The intermolecular bonding of $Rh(CNPh)_4^+$ monomers results from the mixing of higher energy orbitals with the lower energy (filled) d orbitals, resulting in overall stabilization. These bonding interactions give rise to an electronic absorption, at lower energy than the original monomer transition. Similarly, the 600-nm absorption observed in the solid state for Cu^{I}_2ISOIM(EtPh)$_2$(pz) (**15**) is lower in energy, compared to the 440-nm absorption observed for the same compound in solution (Figure 1). Note that in the solid state the higher energy band is at 460 nm. This shift from solution to solid state and the asymmetric nature of the 440-nm solution band suggest that this solution absorption is due to several transitions, one of which may be shifted to lower energy (600 nm) upon interaction with another copper(I). Complexes with apparent copper(I)–copper(I) interactions have not been reported to exhibit notable electronic absorption spectra. Exact assignments of the electronic absorption spectral bands in the copper(I) complexes reported herein await further study.

The solution structure of Cu^{I}_2ISOIM(Etpy)$_2$(pz) (**9**) appears to be similar to that found in the solid state with the absence of the intermolecular Cu–Cu interaction. The pyridine nitrogens do not appear to be bound in benzene solution, since the NMR resonance for the proton on the carbon adjacent to the pyridine nitrogen (py_1, Table I) of Cu^{I}_2ISOIM(Etpy)$_2$(pz) (**9**) occurs at the same position, within experimental error, as the corresponding proton from 2-(2′-aminoethyl)pyridine (i.e., δ 8.44 ± 0.02 ppm from Me_4Si). In fact, all compounds which contain pyridine on the side arms exhibit this resonance at the same position within experimental error (i.e., δ 8.42 ± 0.04 ppm from Me_4Si). The resonance of this proton would be expected to shift downfield upon binding to a copper(I) ion. This effect has been observed for the proton in the 2 position of an imidazole ring, which shifts by 0.4–0.7 ppm downfield upon binding copper(I) to the imidazole ring.[30] Sharp resonances were observed for the pyrazole protons of these compounds (for instance, the doublet at 7.87 ppm and the triplet at 6.43 ppm in Figure 2). This indicates that there is no equilibrium between bound and unbound pyrazole, and hence the pyrazolate bridge must be totally bound to the copper(I) ions or totally dissociated in benzene solutions (unlikely, at best). The 7-azaindolate bridge also appears to be completely bound to the copper ions in benzene solutions, since the resonances for the β_2 aliphatic hydrogens (on the side arms) are split by the unsymmetric bridge (for instance, compound **22** in Table I). Also, the resonance found for the 7-azaindolate protons are very sharp peaks, indicating that no dissociation equilibrium is occurring.

The new copper(I) compounds serve as an interesting series for electrochemical comparisons. Several trends can be observed in Table II. In the following discussion, the formal potentials for the second reduction (E_2^f), eq 4, will be used since these processes were more reversible and slightly more systematic than the E_1^f potentials. The general trends, however, are the same with both processes.

$$Cu^{II}Cu^{I}L^+ + e^- \overset{E_2^f}{\rightleftharpoons} Cu^{I}Cu^{I}L \qquad (4)$$

The first point of interest is the effect of the possible binding sites (i.e., pyridine) in the side arms. The following series of potentials (E_2^f) was observed: Cu^{I}_2ISOIM(EtPh$_2$)$_2$(pz)

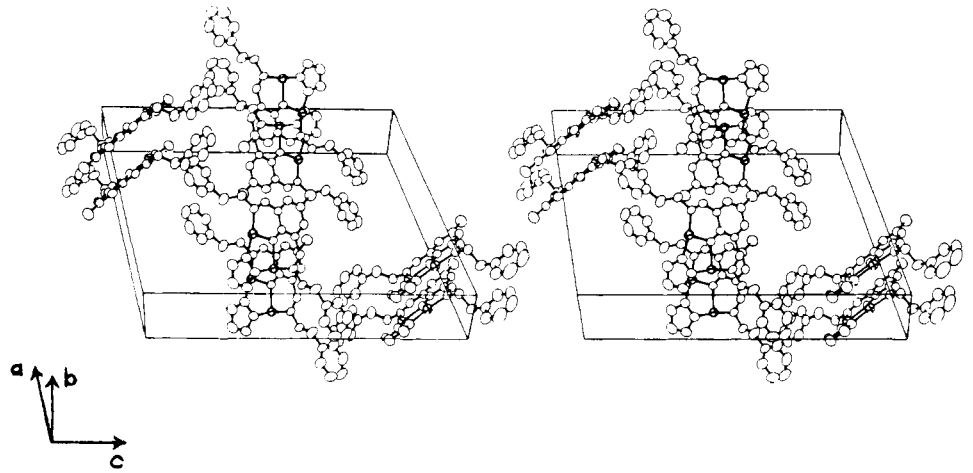

Figure 6. Stereoview illustrating crystal packing of Cu^{I}_2ISOIM(Etpy)$_2$(pz) (**9**). The molecules depicted comprise more than one unit cell, although the edges of only one cell are shown.

Scheme III

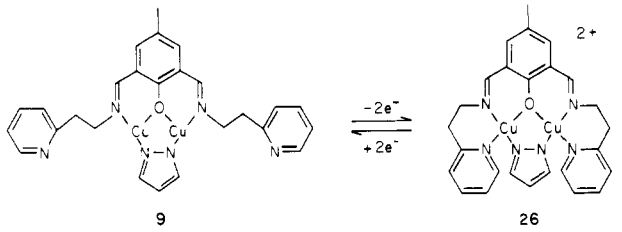

9 26

(**15**, −0.078 V) ≈ Cu^{I}_2ISOIM(MePh)$_2$(pz) (**12**, −0.081 V) ≫ Cu^{I}_2ISOIM(Etpy)$_2$(pz) (**9**, −0.344 V) > Cu^{I}_2ISOIM(Mepy)$_2$(pz) (**6**, −0.452 V). This indicates that the complexes containing the pyridine rings provide a more favorable environment for copper(II) relative to copper(I) when compared to their benzene ring analogues. Since the pyridine nitrogens do not appear to be bound to the copper(I) ions (in solution or in the solid state), the effect of these pyridine rings must be largely on the oxidized copper(II) sites. Hence, it appears that the pyridines bind to the copper ions upon oxidation, **26**, and dissociate from copper(I) upon reduction, **9**, Scheme III. Recall that, in the similar cupric complex, Cu^{II}_2ISOIM(hist)$_2$(OH)$^{2+}$ (**5**), the imidazole nitrogens were shown to be coordinated in the solid-state X-ray structure.[27] It is reasonable that side-arm pyridine nitrogens would also coordinate to copper(II). The above series also indicates that the methylpyridine side arm provides a better environment for copper(II) than does the ethylpyridine side arm. This may be a result of the geometry of the side arms and their relative ability to bind to the copper(II) centers.

The introduction of methyl substituents on the pyrazolate bridges causes an increase in the reduction potential (E_2^{f}) as follows: Cu^{I}_2ISOIM(Mepy)$_2$(Me$_2$pz) (**7**, −0.374 V) > Cu^{I}_2ISOIM(Mepy)$_2$(pz) (**6**, −0.452 V) and Cu^{I}_2ISOIM(MePh)$_2$(Me$_2$pz) (**13**, +0.005 V) > Cu^{I}_2ISOIM(MePh)$_2$(pz) (**12**, −0.081 V). An inductive effect of the methyl groups would stabilize copper(II) relative to copper(I), but the reverse trend is actually observed. The steric bulk of the methyl groups may be responsible for the relative destabilization of copper(II). These methyl groups may inhibit the binding of both pyridine (from the side arms) and DMF (solvent) to the oxidized copper(II) ions by partially blocking the fourth, square-planar binding site around each copper(II). Also, shielding the copper centers from the solvent molecules with hydrophobic groups (such as these methyls) may not allow the polar DMF molecules to efficiently solvate the charged copper(II) species. Relative stabilization of copper(I) also results from more bulky side arms, as reflected in the following series (E_2^{f}): Cu^{I}_2ISOIM(t-Bu)$_2$(pz) (**20**, +0.053 V) > Cu^{I}_2ISOIM(2-Pr)$_2$(pz) (**19**, +0.001 V) > Cu^{I}_2ISOIM(1-Pr)$_2$(pz) (**18**, −0.076 V).

Finally, an electronic effect is observed in the series of compounds which have phenyl rings bonded directly to the imine nitrogens: Cu^{I}_2ISOIM(PhCOMe)$_2$(pz) (**25**, +0.008 V) > Cu^{I}_2ISOIM(Ph)$_2$(pz) (**23**, −0.032 V) > Cu^{I}_2ISOIM(PhNMe$_2$)$_2$(pz) (**24**, −0.048 V). Here, the electron-withdrawing carbonyl substituent results in relative copper(I) stabilization, while the electron-donating amine substituent results in relative copper(II) stabilization. Similar effects of remote substituents have been reported recently for a series of mononuclear copper(II) complexes.[10]

The oxidation/reduction of these compounds in two one-electron steps was the expected behavior for two interacting metal centers.[14,32] This sequential behavior has been observed for the series of binuclear complexes, **27**, recently investigated

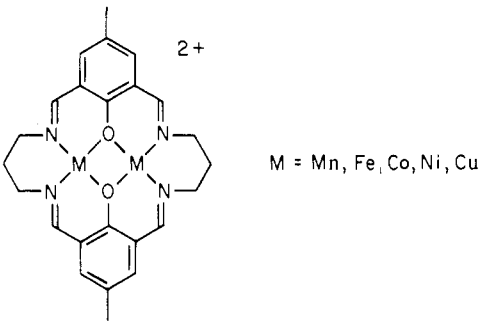

27

in our laboratories.[33] Stepwise oxidation/reduction was also found for many ruthenium(II) dimers, in which closer proximity and greater interactions between the ruthenium centers correlate with a greater separation of the two redox processes (and larger comproportionation constants).[34] That all the new complexes exhibit two one-electron redox waves further suggests that the binuclear compounds are monomeric in solution. Oligomerization would probably result in intermolecular copper–copper interactions leading to more complex electrochemical behavior. Even the complexes with *tert*-butyl side arms, which were designed to inhibit intermolecular interactions, show electrochemical behavior similar to all other compounds. It thus seems likely that all new complexes have comparable solution structures, the most probable having three-coordinate Cu(I).

The average comproportionation constant found for the

binuclear copper complexes in this study (from Table II) was $K = 1.9 \times 10^3$, which is smaller than that found for the macrocyclic binuclear copper complex, **1** ($K = 4 \times 10^6$).[14] This is reasonable since the lower value was observed for the present copper(I) compounds which contain one pyrazolate type bridge and one phenoxide bridge, compared to two phenoxide bridges between the coppers in **1**. The pyrazolate bridge is expected to result in a larger Cu–Cu distance and smaller intramolecular copper intereactions. The oxidized binuclear copper(II) complexes with bridging pyrazolate, such as **26,** Scheme III, were not isolated in the present study, but the relative effects of alkoxide vs. pyrazolate bridges on metal interactions have been demonstrated in similar binuclear copper(II) compounds and the trend was the same as found here.[35]

The nonreactivity of the copper(I) complexes in the present study toward carbon monoxide is an addition to the confusing phenomenon of carbon monoxide binding to copper(I) complexes. In general, copper(I) complexes have been found to bind CO if a fourth coordination site is available.[12,31,36] On the other hand, most four-coordinate copper(I) compounds do not bind CO, with the exception of several square-planar, four-coordinate complexes, which bind CO as a fifth ligand.[13-15] Obviously, the geometry and type of ligands around copper(I) affect the CO binding ability for copper(I). The nature of these effects, however, remains obscure.

Biological Implications

It may not be valid to compare exact reduction potentials of simple metal complexes with those of corresponding protein systems due to varying solvation effects.[37] Nonetheless, analysis of trends or comparisons of approximate potentials may be useful. Within this context the high reduction potentials observed for binuclear copper protein sites have been "mimicked" by the binuclear copper complexes presented in this study. Hence, it is not unreasonable to believe that these proteins utilize only oxygen and/or nitrogen ligands around each copper. Indeed, a three-coordinate copper–ligand environment can be considered for the reduced form of the binuclear site. The nonreactivity of the new compounds toward CO is in contrast to hemocyanin. This does not preclude a three-coordinate reduced binuclear site, since some three-coordinate copper(I) complexes have been shown to bind CO.[12,31,36]

The oxidation/reduction of these compounds in well-separated one-electron steps contrasts with the available electrochemical information on the binuclear protein sites. While no electrochemical data is available on hemocyanin, for both laccase and tyrosinase, a single potential has been associated with the overall two-electron reduction of the binuclear copper site.[6,7,38] Correlations between the electrochemical behavior of the new compounds, **6–25,** and of the proteins is difficult owing to solvation effects, the different techniques employed, possible nonequilibria in the proteins, etc.[37,38] Nonetheless, the electrochemical behavior reported for the new compounds suggests that the two-electron reduction of laccase and of tyrosinase is probably not a simple reduction of two equivalent copper ions strongly interacting through bridging ligands.

Conclusions

Stable binuclear copper(I) complexes have been prepared using binucleating ligands. Several of the new complexes exhibit copper–copper interactions in the solid state, as suggested by a peculiar visible absorption spectrum. This was confirmed for Cu^{I}_2ISOIM(Etpy)$_2$(pz) (**9**) via a complete molecular structure determination. In addition to the copper–copper interaction each copper(I) is bound to one oxygen and two nitrogen ligands. In solution all the new cuprous complexes likely contain three-coordinate copper, which appears to be a quite stable environment for copper(I).

All new complexes exhibit two one-electron redox processes, at well-defined potentials. The highest reduction potentials were observed for complex **21** in which the copper(I) centers are somewhat buried within the hydrophobic substituents. With reduction potentials of $E_1^f = 0.239$ and $E_2^f = 0.080$ V, the ligand environment in **21** represents a substantial improvement on the original square-planar, four-coordinate ligand environment provided by the starting model, **1**. The reason for this high (relative) stability of copper(I) within the new molecules is not obvious. While many three-coordinate mononuclear copper(I) complexes have been isolated employing very soft phosphorus or sulfur donors, very few three-coordinate monuclear (or binuclear) copper(I) complexes have been isolated with nitrogen or oxygen donors.[23,28,39] The binuclear nature of the compounds in this study may be responsible for their stability. Perhaps the second copper serves to anchor the binucleating ligands, promoting a favorable three-coordinate environment around each copper(I).

Relatively high reduction potentials on the order exhibited by these complexes (and by the binuclear protein site) may be necessary for reversible oxygen binding.[40] Unfortunately these complexes have thus far reacted irreversibly toward oxygen. We are presently investigating modifications on the side arms and their effect on the nature of the oxygenation reaction.

Experimental Section

Materials. All chemicals were reagent grade and were used as received unless otherwise noted. Copper(II) tetrafluoroborate, ground to a powder and then dried for several days in vacuo (25 °C), was used as $Cu(BF_4)_2 \cdot 6H_2O$. Tetrabutylammonium perchlorate (TBAP, Southwestern Analytical Chemicals) was dried exhaustively in vacuo (25 °C) before use. Reagent grade *N,N*-dimethylformamide (DMF) was dried over $MgSO_4$ and 4A molecular sieves for 24 h and then vacuum distilled. 2-Hydroxy-5-methylisophthalaldehyde was prepared by a modification of the literature method.[41] Tetra(acetonitrile) copper(I) tetrafluoroborate was also prepared by the published method.[42]

Cu^{II}_2ISOIM(Mepy)$_2$OH(BF$_4$)$_2$·CH$_3$OH·H$_2$O (3). Aminomethylpyridine (0.44 mL, 4 mmol) was added to a solution of 2-hydroxy-5-methylisophthalaldehyde (0.33 g, 2 mmol) in methanol (50 mL). The resulting yellow solution was boiled at reflux for 1 h, after which $Cu(BF_4)_2 \cdot 6H_2O$ (1.38 g, 4 mmol) was added. The resulting blue-green solution was refluxed for 45 min. Removal of the solvent (methanol) using a rotary evaporator gave a blue-green solid, which upon recrystallization from methanol yielded blue-green crystals of **3**. These crystals were washed with methanol followed by diethyl ether and dried under vacuum for several hours. Anal. ($C_{22}H_{26}N_4O_4Cu_2B_2F_8$) C, H, N, Cu.

Cu^{II}_2ISOIM(Etpy)$_2$OH(BF$_4$)$_2$·CH$_3$CH$_2$OH (4). 2-(2′-Aminoethyl)pyridine (0.50 mL, 4 mmol) was added to a solution of 2-hydroxy-5-methylisophthalaldehyde (0.33 g, 2 mmol) in ethanol (25 mL). The resulting yellow solution was boiled at reflux for 5 min and then $Cu(BF_4)_2 \cdot 6H_2O$ (1.38 g, 4 mmol) was added to give a green solution. After boiling for 5 min, this solution was allowed to cool slowly to 4 °C, and the resulting blue-green solid was collected and recrystallized from ethanol to give blue-green crystals of **4**. The product was washed with ethanol followed by diethyl ether and dried under vacuum for several hours. Anal. ($C_{25}H_{30}N_4O_3Cu_2B_2F_8$) C, H, N; Cu: calcd, 17.3; found, 18.0.

Cu^{II}_2ISOIM(hist)$_2$OH(BF$_4$)$_2$·H$_2$O (5). Histamine (0.44 g, 4 mmol) was added to a solution of 2-hydroxy-5-methylisophthalaldehyde (0.33 g, 2 mmol) in methanol (50 mL). The resulting yellow-orange solution was boiled at reflux for 15 min, and then $Cu(BF_4)_2 \cdot 6H_2O$ (1.38 g, 4 mmol) was added to give a green solution. The solution was reduced to a small volume (~10 mL) using a rotary evaporator, and the resulting green solid was collected by vacuum filtration. Recrystallization of this solid from ethanol gave light blue-green needles of **5**. The product was collected and washed with ethanol followed by diethyl ether, and then dried in vacuo for several hours. Anal. ($C_{19}H_{24}N_8O_3Cu_2B_2F_8$) C, H, N; Cu: calcd, 18.6; found, 19.3.

Cuprous Compounds. The series of copper(I) compounds **6–25** was synthesized in the manner described below for Cu^{I}_2ISOIM(Etpy)$_2$(pz) (**9**), with the following modifications. The appropriate amine

(RNH_2) and bridge (XH) were used to provide the R and X groups listed in Table I. The initial imine condensation was slow for the aromatic amines, and the amine and dialdehyde were allowed to react overnight, in refluxing acetonitrile, in the synthesis of **23–25.** Compounds **7, 10, 13, 16,** and **23–25** were recrystallized with DMF instead of CH_3CN. Compounds **20–22** were recrystallized from heptane instead of acetonitrile.

Cu^I_2ISOIM(Etpy)$_2$(pz) (9). The following was performed under helium in a Vacuum Atmospheres Dri-Lab inert atmosphere chamber. 2-(2′-Aminoethyl)pyridine (0.24 mL, 2 mmol) was added to a solution of 2-hydroxy-5-methylisophthalaldehyde (0.16 g, 1 mmol) in acetonitrile (15 mL). The resulting yellow solution was heated at reflux for 15 min and then cooled to the ambient temperature. Pyrazole (0.07 g, 1 mmol) and sodium methoxide (0.11 g, 2 mmol) were added to the solution, and after stirring briefly $Cu(CH_3CN)_4BF_4$ (0.63 g, 2 mmol) was added to give a brown solution and a brown precipitate. This mixture was boiled at reflux for 15 min, and then the acetonitrile was removed by evaporation under vacuum. The brown solid was dissolved in hot toluene (30 mL), leaving behind a white solid ($NaBF_4$) upon vacuum filtration. The toluene was then removed from the filtrate by evaporation under vacuum to yield a brown solid. Recrystallization from acetonitrile gave brown *needles,* **9.** The product was collected by vacuum filtration, washed with acetonitrile, and dried for several hours in vacuo. Anal. ($C_{26}H_{26}N_6OCu_2$) C, H, N, Cu.

Physical Measurements. Sample preparation for physical studies on the air-sensitive materials was accomplished in a Vacuum Atmospheres Dri-Lab inert atmosphere chamber, under a helium atmosphere. Helium-saturated spectroquality solvents were used for solution studies.

Magnetic susceptibility measurements were done on powdered samples at the ambient temperature using a Cahn Instruments Faraday balance. The calibrant utilized was $HgCo(SCN)_4$, and diamagnetic corrections were made using Pascal's constants.

Electronic spectra were recorded on a Cary 14 spectrophotometer. Solid-state spectra were obtained from Nujol mulls on filter paper against a Nujol-saturated filter paper as a blank.

Infrared spectra were recorded on a Beckman IR-12 infrared spectrophotometer. Solid-state spectra were obtained from Nujol mulls pressed between KBr plates. Solution spectra were obtained using calcium fluoride solution cells (path length of 1 mm).

Proton magnetic resonance spectra were recorded on a Varian EM390 spectrophotometer at 90 MHz (34 °C). The solvent utilized was benzene-d_6 containing Me_4Si as the reference.

Mass spectra and elemental analyses were performed by the Caltech Microanalytical Laboratory.

Electrochemistry. A Princeton Applied Research (PAR) Model 174A polarographic analyzer was used for cyclic voltammetry and differential pulse voltammetry. For display purposes, a Hewlett-Packard 7004B X-Y recorder was utilized. The apparatus used for constant-potential electrolysis (CPE) consisted of a PAR Model 173 potentiostat-galvanostat coupled with a Model 179 digital coulometer.

Cyclic voltammetry was done in a single compartment cell with a volume of ca. 5 mL. In all solvents the supporting electrolyte was 0.1 M TBAP. The working electrode consisted of a platinum button electrode or a hanging mercury drop electrode. In all cases, the auxiliary electrode was a coiled platinum wire and the reference electrode consisted of a silver wire immersed in an acetonitrile solution containing $AgNO_3$ (0.01 M) and TBAP (0.1 M), all contained in a 9-mm glass tube fitted on the bottom with a fine porosity sintered glass frit. The apparatus employed for constant-potential electrolysis was similar, except that a two-compartment H cell was used to isolate the auxiliary electrode from the working compartment. A platinum gauze was used as the working electrode for CPE.

All potentials are reported vs. the normal hydrogen electrode, NHE. This was accomplished by the use of an internal reference redox couple, namely, ferrocene, for which the formal potential is reported to be +0.400 V vs. NHE in water.[16] It has been proposed that the ferrocene reduction potential changes very little in different solvents, and hence it is a good solvent-independent redox couple.[16] Experimentally, small amounts (ca. 10^{-3} M) of ferrocene were added to solutions containing the compounds of interest and formal potentials for both couples were measured under the same conditions.

X-ray Data Collection and Reduction. Acicular crystals of **9** were grown by slow evaporation of an acetonitrile solution under helium. Preliminary oscillation and Weissenberg photographs showed the space group to be $P2_1/c$ (no. 14) uniquely defined by its extinctions.

A crystal of dimensions 0.04 × 0.08 × 0.33 mm (which had been cut from a larger needle) was mounted on a Syntex $P2_1$ four-circle diffractometer for data collection. No attempt was made to protect the crystal from atmospheric oxygen as no air sensitivity had been exhibited in the solid state. Cell parameters were determined by a least-squares fit to 15 automatically centered reflections with $2\theta > 56°$. The resulting parameters are given in Table III. Intensity data were collected from two octants using θ–2θ scans to a maximum 2θ of 130°. The scan range extended from 1° below the Cu $K\alpha_1$ 2θ value to 1° above the Cu $K\alpha_2$ value, and the scan rate was 1°/min, with the total background counting time equal to the total scan time. Three check reflections were measured after every 50 reflections to monitor the crystal and instrument stability.

Because the check reflections showed an overall drop in intensity of 5% during the course of data collection, the data was scaled in 11 groups according to the average intensity in each group of one of the check reflections (002). Lorentz and polarization corrections were then applied. Standard deviations of intensities were calculated using the formula

$$\sigma^2(I) = [S + (B1 + B2) + (dS)^2]/(Lp)^2$$

where S, $B1$, and $B2$ are the scan and two background counts and d was taken as 0.02.[43] Absorption corrections were calculated by the method of Gaussian quadrature.[44] After symmetry-extinct reflections were deleted and equivalent reflections averaged, there remain 4269 unique data ($3390 > 0$; a rather high percentage of the high 2θ data was "unobserved").

Solution and Refinement of the Structure. With the exception of C. K. Johnson's ORTEP program, all computer programs were from the CRYM system of crystallographic programs. Literature values were used for the scattering factors for Cu^+, O, N, and C,[45] the real part of the anomalous dispersion correction for copper[45] and for the H scattering factors.[46] The function minimized in the least-squares refinement was $\Sigma w(|F_o|^2 - |k'F_c|^2)^2$, where the weight $w = 1/\sigma^2(F_o^2)$, and F_o and F_c are the observed and calculated structure factors.

The positions of all nonhydrogen atoms were found using standard Patterson–Fourier techniques. Least-squares refinement with these atoms and isotropic temperature factors led to $R = \Sigma||kF_o| - |F_c||/\Sigma|kF_o| = 0.087$ (for those reflections with $F_o^2 > 2\sigma$). Use of anisotropic temperature factors for all nonhydrogen atoms lowered R to 0.062. The 26 hydrogen atoms were located by difference map techniques. Each was assigned a fixed isotropic temperature factor equal to 1.0 Å^2 greater than that for the carbon atom to which it was bound. Hydrogen positional parameters were refined. The final refinement was by blocked-matrix least squares with all positional parameters in one matrix and the anistropic thermal parameters and scale factor in another. No data were omitted from this refinement. The final R was 0.042 for the 2620 reflections with $F_o^2 > 2\sigma$; R for all data was 0.063. The final goodness of fit, $\Sigma w(k^2F_o^2 - F_c^2)^2/(n - p)$, was 2.85, where $n = 4269$ is the number of observations and $p = 394$ is the number of parameters. The largest feature in the final difference Fourier map was a peak of height 0.96 e Å^{-3}, located approximately 0.7 Å from Cu2 in the positive y direction. The second highest peak (0.87 e Å^{-3}) was not in a position of chemical significance (between the pyrazole groups of neighboring molecules). Final parameters and interatomic distances and angles are presented in Tables IV–VII.

Acknowledgment. We appreciate helpful discussions from T. J. Smith and financial assistance from the National Institutes of Health (Grant PHS AM18319-04) and the International Copper Research Association.

Supplementary Material Available: A listing of structure factor amplitudes (16 pages). Ordering information is given on any current masthead page.

References and Notes

(1) Lontie, R. In "Inorganic Biochemistry", Eichhorn, G. I., Ed.; American Elsevier: New York, 1973; p 344.
(2) (a) Mason, H. S. *Annu. Rev. Biochem.* **1965,** *35,* 595–634. (b) Vanneste, W. H.; Zuberbühler, A. In "Molecular Mechanisms of Oxygen Activation", Hayaishi, O., Ed.; Academic Press: New York, 1974; p 371.
(3) (a) Fee, J. A. *Struct. Bonding (Berlin)* **1975,** *23,* 1–60. (b) Vänngård, T. I.

In "Biological Applications of Electron Spin Resonance Spectroscopy", Swartz, H. M., Bolton, J. R., Borg, D. C., Eds.; Wiley: New York, 1972; p 411.
(4) See: Wurzbach, J. A.; Grunthaner, P. J.; Dooley, D. M.; Gray, H. B.; Grunthaner, F. J.; Gay, R. R.; Solomon, E. I. *J. Am. Chem. Soc.* **1977**, *99*, 1257–1258, and references cited therein.
(5) Solomon, E. I.; Dooley, D. M.; Wang, R.; Gray, H. B.; Cerdonio, M.; Mogno, F.; Romani, G. L. *J. Am. Chem. Soc.* **1976**, *98*, 1029–1031.
(6) Makino, N.; McMahill, P.; Mason, H. S.; Moss, T. H. *J. Biol. Chem.* **1974**, *249*, 6062–6066.
(7) (a) Reinhammar, B. R. M. *Eur. J. Biochem.* **1971**, *18*, 463–468. Reinhammar, B. R. M.; Vänngård, T. I. *Biochim. Biophys. Acta* **1972**, *275*, 245–259. (b) Farver, O.; Goldberg, M.; Lancet, D.; Pecht, I. *Biochem. Biophys. Res. Commun.* **1976**, *73*, 494–500.
(8) For example, see: Amundsen, A. R.; Whelan, J.; Bosnich, B. *J. Am. Chem. Soc.* **1977**, *99*, 6730–6739. Simmons, M. G.; Wilson, L. J. *J. Chem. Soc., Chem. Commun.* **1978**, 634–636. Bulkowski, J. E.; Burk, P. L.; Ludmann, M. F.; Osborne, J. A. *Ibid.* **1977**, 498–499. Lehn, J. M.; Pine, S. H.; Watanabe, E.; Willark, A. K. *J. Am. Chem. Soc.* **1977**, *99*, 6766–6768. Alberts, A. H.; Annunziata, R.; Lehn, J. M. *Ibid.* **1977**, *99*, 8502–8504.
(9) Arcus, C. S.; Wilkinson, J. L.; Mealli, C.; Marks, T. J.; Ibers, J. A. *J. Am. Chem. Soc.* **1974**, *96*, 7564–7565. Mealli, C.; Arcus, C. S.; Wilkinson, J. L.; Marks, T. J.; Ibers, J. A. *Ibid.* **1976**, *98*, 711–718.
(10) Yokoi, H.; Addison, A. W. *Inorg. Chem.* **1977**, *16*, 1341–1349.
(11) Fenton, D. E.; Lintvedt, R. L. *J. Am. Chem. Soc.* **1978**, 200, 6367–6375.
(12) Gagné, R. R.; Gall, R. S.; Lisensky, G. C.; Marsh, R. E.; Speltz, L. M. *Inorg. Chem.* **1979**, *18*, 771–781.
(13) Gagné, R. R. *J. Am. Chem. Soc.* **1976**, *98*, 6709–6710. Gagné, R. R.; Allison, J. L.; Gall, R. S.; Koval, C. A. *Ibid.* **1977**, *99*, 7170–7178.
(14) Gagné, R. R.; Koval, C. A.; Smith, T. J. *J. Am. Chem. Soc.* **1977**, *99*, 8367–8368. Gagné, R. R.; Koval, C. A.; Smith, T. J.; Cimolino, M. C., *J. Am. Chem. Soc.* **1979**, *101*, 4571–4580.
(15) Gagné, R. R.; Allison, J. L.; Lisensky, G. C. *Inorg. Chem.* **1978**, *17*, 3563–3571. Gagné, R. R.; Allison, J. L.; Ingle, D. M., *Inorg. Chem.*, in press.
(16) Bauer, D.; Breant, M. In "Electroanalytical Chemistry", Bard, A. J., Ed.; Marcel Dekker: New York, 1975; Vol. 8, pp 282–344.
(17) Attempts to isolate $Cu^{II}_2ISOIM(Mepy)_2(pz)^{2+}$ directly from Cu(II) starting materials led only to $Cu^{II}_2ISOIM(Mepy)(OH)^{2+}$ (**3**).
(18) All electrochemical measurments were made without the use of *iR* compensation. The cyclic voltammetric peak-to-peak separations are comparable to those we have observed for other chemically reversible redox couples involving polydentate ligands.[13,14] For comparison purposes, under the cyclic voltammetric conditions utilized ferrocene was observed to give peak-to-peak separations of 70–80 mV.
(19) The separation between planes of carbon atoms in graphite is 3.35 Å, for example.[20] In a recent series of crystal structures of Schiff bases akin to the ligand in the present structure, interplanar distances of 3.42–3.50 Å were found.[21] See also: Herbstein, F. H. In "Perspectives in Structural Chemistry", Dunitz, J. D., Ibers, J. A., Eds.; Wiley: New York, 1972; Vol. 4, p 166.
(20) Cotton, F. A.; Wilkinson, G. "Advanced Inorganic Chemistry"; Interscience: New York, 1972; p 288.
(21) Moustakali-Mavridis, I.; Hadjoudis, E.; Mavridis, A. *Acta Crystallogr., Sect. B* **1978**, *34*, 3709–3715.
(22) Some of the shorter Cu(I)–N distances that have been reported are as follows: 1.937–1.943 Å in [1,1-difluoro-4,5,11,12-tetramethyl-1-bora-3,6,10,13 - tetraaza - 2,14-dioxacyclotetradeca-3,5,10,12-tetraenato]-copper(I), which contains copper in a distorted square-planar geometry;[15] 1.946 and 1.948 Å for the nonbridging pyrazole groups in bis[(hydrotris(1-pyrazolyl)borato)copper(I)], which contains copper in a distorted tetrahedral geometry;[9] 1.97–2.02 Å in tris(2-picoline)copper(I) perchlorate, in which copper is three coordinate, with a distorted trigonal-planar geometry.[23] One structure that does have a Cu(I)–N bond about as short as some of those in the present structure is the dimer of diazoaminobenzenecopper(I). This contains two-coordinate copper, with Cu–N distances of 1.898 and 1.939 Å (also a Cu–Cu distance of 2.451 Å).[24]
(23) Lewin, A. H.; Michl, R. J.; Ganis, P.; Lepore, U. *J. Chem. Soc., Chem. Commun.* **1972**, 661–662.
(24) Brown, I. D.; Dunitz, J. D. *Acta Crystallogr.* **1961**, *14*, 480–485.
(25) Structural and electronic factors influencing copper reduction potentials have been documented: Patterson, G. S.; Holm, R. H. *Bioinorg. Chem.* **1975**, *4*, 257–275.
(26) Grzybowski, J. J.; Merrell, P. H.; Urbach, F. L. *Inorg. Chem.* **1978**, *17*, 3078–3082.
(27) Gagné, R. R.; McCool, M.; Marsh, R. E.; Kreh, R. P., unpublished results.
(28) For example, see: Camus, A.; Marsich, N.; Nardin, G.; Randaccio, L. *Inorg. Chim. Acta* **1977**, *23*, 131–144. Jardine, F. *Adv. Inorg. Chem. Radiochem.* **1975**, *17*, 115–163. Mehrotra, P. K.; Hoffmann, R. *Inorg. Chem.* **1978**, *17*, 2187–2189, and references cited therein.
(29) Mann, K. R.; Gordon, J. G.; Gray, H. B. *J. Am. Chem. Soc.* **1975**, *97*, 3553–3555. Lewis, N. S.; Mann, K. R.; Gordon, J. G.; Gray, H. B. **1976**, *98*, 7461–7463. Mann, K. R.; Lewis, N. S.; Williams, R. M.; Gray, H. B.; Gordon, J. G. *Inorg. Chem.* **1978**, *17*, 828–834.
(30) Suguira, Y. *Inorg. Chem.* **1978**, *17*, 2177–2182. We have also observed a 0.13-ppm downfield shift of the proton on the carbon adjacent to the pyridine nitrogen of *N,N,N',N'*-tetrakis(2-pyridylmethyl)ethylenediamine (TPEN) upon binding of Cu(I) to this pyridine ring.[31]
(31) Gagné, R. R.; McCool, M.; Marsh, R. E.; Ingle, D. M.; Kreh, R. P., unpublished results.
(32) A curious exception to the stepwise electrochemistry exhibited by interaction metals is that reported for a series of binuclear triketonatocopper(II) complexes.[11]
(33) Gagné, R. R.; Spiro. C. L., unpublished results.
(34) (a) Creutz, C.; Taube, H. *J. Am. Chem. Soc.* **1969**, *91*, 3988–3989; **1973**, *95*, 1086–1094. (b) Weaver, T. R.; Meyer, T. J.; Adeyemi, S. A.; Brown, G. M.; Eckberg, R. P.; Hatfield, W. E.; Johnson, E. C.; Murray, R. W.; Untereker, D. *Ibid.* **1975**, *97*, 3039–3048. (c) Callahan, R. W.; Keene, F. R.; Meyer, T. J.; Salmon, D. J. *Ibid.* **1977**, *99*, 1064–1073.
(35) Robson, R. *Inorg. Nucl. Chem. Lett.* **1970**, *6*, 125–128.
(36) Bruce, M. I.; Ostazewski, A. P. *J. Chem. Soc., Dalton Trans.* **1973**, 2433–2436. Churchill, M. R.; DeBoer, B. G.; Rotella, F. J.; Abu Salah, O. M.; Bruce, M. I. *Inorg. Chem.* **1975**, *14*, 2051–2056.
(37) Hill, C. L.; Renaud, J.; Holm, R. H.; Mortenson, L. E. *J. Am. Chem. Soc.* **1977**, *99*, 2549–2557.
(38) Farver, O.; Goldberg, M.; Wherland, S.; Pecht, I. *Proc. Natl. Acad. Sci. U.S.A.* **1978**, *75*, 5245–4249.
(39) Ellen, P.; Bradley, D.; Hursthouse, M.; Meek, D. *Coord. Chem. Rev.* **1977**, *24*, 1–95.
(40) Reversibility of oxygenation in mononuclear cobalt complexes was shown to be related to reduction potentials: Carter, M. J.; Rillema, D. P.; Basolo, F. *J. Am. Chem. Soc.* **1974**, *96*, 392–400.
(41) Ullmann, F.; Brittner, K. *Chem. Ber.* **1909**, *42*, 2539–2548.
(42) Hathaway, B. I.; Holah, D. G.; Postlethwaite, J. D. *J. Chem. Soc.* **1961**, 3215–3218.
(43) Peterson, S. W.; Levy, H. A. *Acta Crystallogr.* **1957**, *10*, 70–76.
(44) Busing, W. R.; Levy, H. A. *Acta Crystallogr.* **1975**, *10*, 180–182.
(45) "International Tables for X-ray Crystallography", Vol. III; Kynoch Press: Birmingham, England, 1962.
(46) Stewart, R. F.; Davidson, E. R.; Simpson, W. T. *J. Chem. Phys.* **1965**, *42*, 3175–3187.